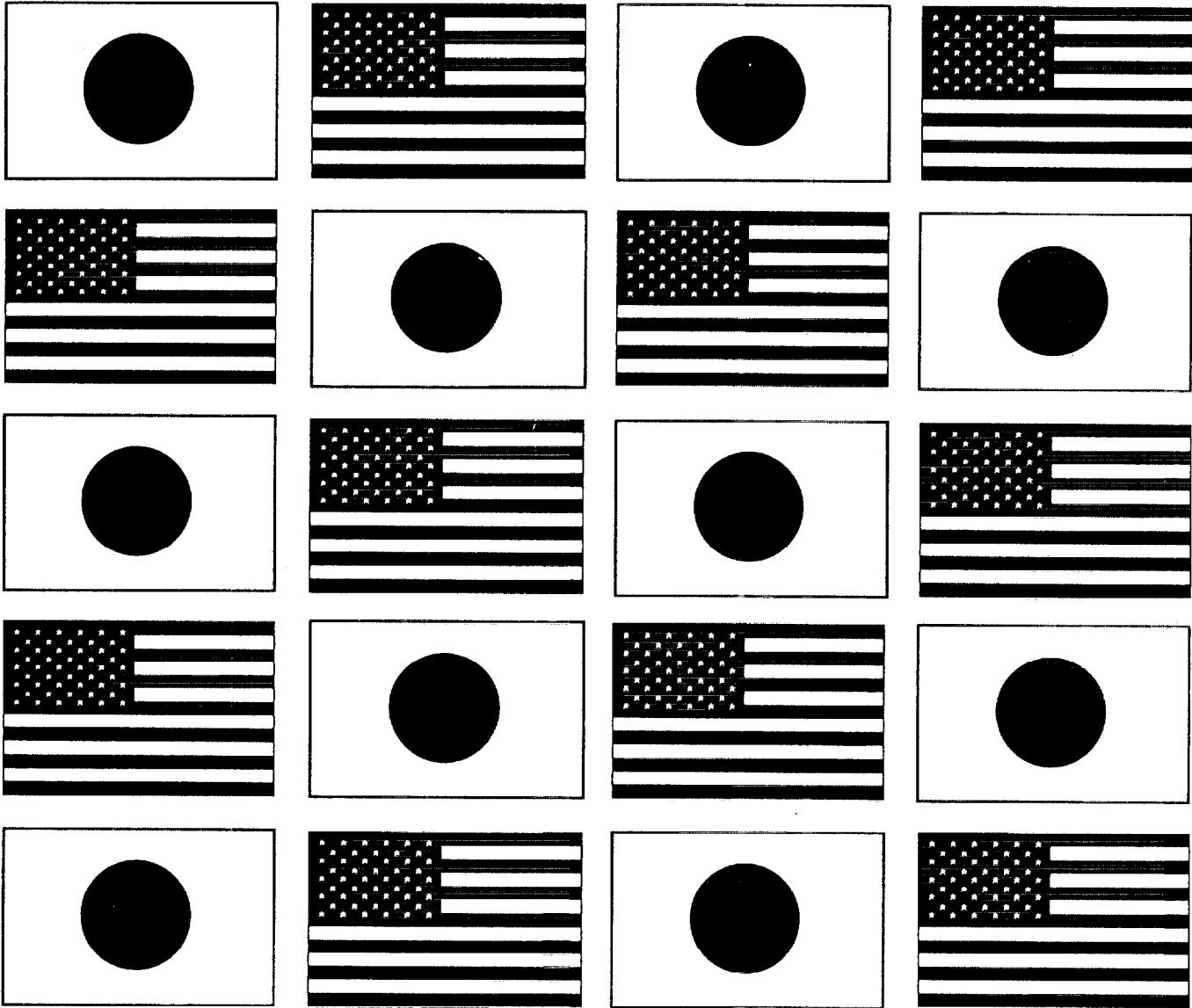


Wind and Seismic Effects

Proceedings of the 30th Joint Meeting

NIST SP 931



U.S. DEPARTMENT OF COMMERCE
Technology Administration
National Institute of Standards and Technology

Wind and Seismic Effects

NIST SP 931

**PROCEEDINGS OF
THE 30TH JOINT
MEETING OF
THE U.S.-JAPAN
COOPERATIVE PROGRAM
IN NATURAL RESOURCES
PANEL ON WIND AND
SEISMIC EFFECTS**

Issued August 1998

**Noel J. Raufaste
EDITOR**

**Building and Fire Research Laboratory
National Institute of Standards and Technology
Gaithersburg, MD 20899**



**U.S. DEPARTMENT OF COMMERCE
William M. Daley, Secretary**

**TECHNOLOGY ADMINISTRATION
Gary R. Bachula, Acting Under Secretary for Technology**

**National Institute of Standards and Technology
Raymond G. Kammer, Director**

EARTHQUAKE ENGINEERING

Strong Motion from Surface Waves in Deep Sedimentary Basins

by

William B. Joyner¹

ABSTRACT

It is widely recognized that long-period surface waves generated by conversion of body waves at the boundaries of deep sedimentary basins make an important contribution to strong ground motion. The factors controlling the amplitude of such motion, however, are not widely understood. Compared to the body wave, the velocity of the surface wave is much less, and, as a result, the curvature of the wavefront and the geometric spreading are much less. The surface wave behaves approximately as if it were generated by a line source in a two-dimensional medium. On the other hand the low-Q basin sediments produce significant anelastic attenuation, even at relatively long periods. A study of pseudovelocity response spectra of records of the 1971 San Fernando and 1994 Northridge earthquakes at sites in the Los Angeles Basin shows that late-arriving surface waves with group velocities of about 1 km/sec dominate the ground motion for periods of 3 sec and longer. The rate of amplitude decay for these waves is less than for the body waves and depends significantly on period, with smaller decay for longer periods. The amplitude can be modeled by anelastic attenuation with decay proportional to the exponential of distance multiplied by an attenuation coefficient. Methods for estimating the response spectral amplitudes for these waves in future earthquakes are presented based on either the San Fernando or Northridge data. The response spectral amplitude of surface waves from the Northridge earthquake is less than from the San Fernando earthquake by factors as large as four. The surprisingly large difference between the San Fernando and Northridge earthquakes can be explained, at least in part, by directivity. Estimates of response values in future earthquakes based on the two different data sets give a sense of the range of

possibilities. These estimates are based on data from the Los Angeles Basin, but, in the absence of other data, they could be applied to sites in other deep Quaternary basins. The results presented in this paper indicate that inclusion of anelastic attenuation may be essential in modeling ground motion in deep sedimentary basins. Future progress in understanding strong motion from basin surface waves calls for attention to faithful recording of the long-period components of ground motion and to recording motion for times long enough to include the late-arriving surface waves.

1. INTRODUCTION

The importance of surface waves for long-period strong earthquake ground motion has long been recognized. Hanks (1975) examined displacement time series obtained by double integration of accelerometer records from the 1971 San Fernando, California, earthquake and showed that surface waves were a significant component of the long-period motion. Surface waves in the San Fernando earthquake were also studied by Lui and Heaton (1984) and by Vidale and Helmberger (1988) who showed that the surface waves were generated by conversion from body waves at the margins of deep sedimentary basins.

The factors controlling the amplitude of surface waves generated by conversion of body waves at basin margins are not widely understood. The amplitude of surface waves is commonly said to decay as the one-half power of distance. That statement is only true for laterally homogeneous media and then only in the frequency domain. The decay in the time domain is greater because of dispersion. With

¹ U.S. Geological Survey, 345 Middlefield Road MS 977, Menlo Park, CA 94025

lateral heterogeneity, as with a surface wave generated at the edge of a basin, the situation is very different. As shown in Figure 1, because the velocity of the surface wave is much less than the body wave, the curvature of the wavefront for the surface wave is much less and the geometric spreading of the surface wave is thereby much reduced. In Figure 1 the reduction would be greater if the boundary were concave inward. To a first approximation the wave behaves as if it were generated by a line source in a two-dimensional medium. On the other hand, the low- Q basin sediments produce significant anelastic attenuation. In this paper strong-motion data from the 1971 San Fernando, California, and the Northridge, California, earthquakes are examined to clarify the role of surface waves and the factors controlling their amplitude.

2. DATA

The focus of this study was surface waves in deep sedimentary basins generated by earthquakes outside the basin. The data used were strong-motion records of the San Fernando and Northridge earthquakes recorded at sites in the Los Angeles Basin (Figure 2). For the purposes of this paper, the boundary of the Los Angeles Basin were taken as the 300 m contour of depth to crystalline basement as determined by adjusting the subsea elevation contours on the map by Yerkes *et al.* (1965) for the effect of topography. With that definition of the Basin boundary, the San Fernando and Northridge earthquakes lie outside the Basin.

The San Fernando data were taken from the CD-ROM by Seekins *et al.* (1992). The horizontal components were rotated to north and east, approximately perpendicular and parallel, respectively, to the northern boundary of the basin. The records were then processed specifically for this study using as lowcut filter a second-order bidirectional Butterworth filter (Converse, 1992) with a cutoff at 0.125 Hz. The locut filter is similar to that recommended by Hanks (1975). Velocity time series were plotted in order of increasing distance from the source, and records with duration judged

insufficient to record the surface waves were eliminated, leaving 56 three-component records. The Northridge data were taken from the California Strong Motion Instrumentation Program and from the Los Angeles Strong Motion Accelerograph Network operated by the University of Southern California. Corrected data were obtained from processing by the network operators. Both operators employ a lowcut filter that is a ramp in the frequency domain. Records were excluded from this study if the frequency at the upper end of the ramp exceeded 0.16 Hz. Twelve three-component records remained after the exclusions. As with the San Fernando records the horizontal components were rotated to north and east.

3. PRELIMINARY ANALYSIS

In order to assess the contribution of surface waves to ground motion, pseudovelocity response spectra for 5 percent damping were computed for each record and the time of maximum response was determined for each oscillator period and each record. A regression analysis was performed between the time of maximum response and the closest horizontal distance from the recording station to the vertical projection on the surface of the earth of the fault rupture that generated the earthquake. The resulting regression coefficient is plotted against oscillator period for the San Fernando earthquake on Figure 3 and the Northridge earthquake on Figure 4. The regression coefficient represents the group slowness, that is, the reciprocal of the group velocity, of the seismic phase that carries the highest amplitude for each period. More precisely, the coefficient is the group slowness relative to the slowness of the triggering phase. An examination of the accelerograms shows that some of the records triggered on the P -wave and some on the S -wave, but it does not matter because the body-wave slownesses are negligible compared to the surface-wave slownesses. Group velocities and slownesses are usually measured by noting the time of the peak of the envelope of narrow-band-filtered seismograms. The approach used here should give similar results and has the advantage of employing quantities of

engineering significance. Figures 3 and 4 show that for periods up to about 0.75 sec body waves with relative slownesses near zero carry the maximum amplitude. At periods of 3.0 sec and greater the relative slowness is nearly 1 sec/km, representing surface waves whose absolute slowness may exceed 1 sec/km. Between periods of about 0.75 and 3.0 sec the regression coefficients take on intermediate values. These probably do not represent a seismic phase of intermediate slowness but rather a situation where the maximum amplitude is carried by the body waves on some records and by the surface waves on others. Using the distance dependence of the time of maximum amplitude to distinguish surface waves and body waves is a strategy employed by Hanks and McGuire (1981).

Regression analysis was also performed between the logarithm of the pseudovelocity response and the logarithm of distance. The regression coefficient is plotted against period on Figure 5 for the San Fernando earthquake and on Figure 6 for the Northridge earthquake. The surface waves at periods of 3.0 sec and greater have a decay rate generally less than the body waves at periods 0.75 sec and less. Note that the decay rate of the surface waves decreases sharply with period, suggesting that the decay represents anelastic attenuation, not geometric spreading.

4. EQUATIONS

The results of the last section suggest that the pseudovelocity amplitudes of the surface waves could be represented by an equation of the form

$$y = \frac{a}{R_E} \exp(-bR_B) \quad (1)$$

where y is the pseudovelocity response, R_E is the distance from the source to the edge of the basin, R_B is the distance from the edge of the basin to the recording site, and a and b are parameters chosen to fit the data. Values of R_E

and R_B are obtained by constructing the line between the recording site and the closest point on the vertical projection of the fault rupture on the earth's surface. The intersection point of the line with the basin boundary is noted, and the distance between the intersection point and the closest point on the vertical projection of the fault rupture is denoted by D_E . $R_E = \sqrt{(D_E^2 + 25)}$. R_B is the distance between the intersection point and the recording site. Values of a and b derived by fitting the San Fernando data and the Northridge data separately are given in Table 1. Values of Q implied by the values obtained for b are given in Table 2, along with one-standard-deviation ranges, for an assumed phase velocity of 1 km/sec. The ratios between observed values and values predicted by equation (1) are shown on Figure 7 for the perpendicular component of the San Fernando earthquake at periods of 3 to 6 sec. Data for the other components of the San Fernando earthquake and for the Northridge earthquake are similar. The standard deviation of the natural logarithm of the ratio between observed and predicted values ranges between 0.3 and 0.5. Figure 8 shows the values predicted by equation (1) with a and b fitted to data from the perpendicular component for the San Fernando (S) and Northridge (N) earthquakes. Also shown on Figure 8 for comparison are values predicted by two attenuation relationships derived from the general strong-motion data set. Figure 9 shows the corresponding results for the parallel component. The values predicted from fits to the San Fernando data are larger than predicted by the two attenuation relationships by as much as a factor of four. The values predicted from fits to the Northridge data are much less than those from fits to the San Fernando earthquake. This difference between the San Fernando and Northridge data is surprisingly large, but it can be explained, at least in part, by directivity.

Estimates of pseudovelocity response obtained from equation (1) fit to the San Fernando data can be extrapolated to other sites and other earthquakes by multiplying the result from equation (1) by the factor $f(\mathbf{M}, R_E) / f(6.6, 23)$, where $f(\mathbf{M}, R)$ is an appropriate attenuation relationship for pseudovelocity response in

terms of moment magnitude M and distance R in km, 6.6 being the moment magnitude of the San Fernando earthquake and 23 km the average distance between the source and the basin edge for the San Fernando records. The corresponding estimates for fits to the Northridge data can be obtained by multiplying the results from equation (1) by the factor $f(M, R_E) / f(6.7, 17)$. Estimates derived from the San Fernando and Northridge data would give some sense of the range of values that might occur in a future earthquake. Such estimates, though based on data from the Los Angeles Basin, could be applied to sites in other deep Quaternary basins where data is not available.

5. CONCLUSIONS AND RECOMMENDATIONS

The results presented here show that in a deep sedimentary basin such as the Los Angeles Basin the ground motion at periods of 3 to 6 sec is dominated by surface waves. Methods are described for estimating response spectral values for such motion. Estimates made using data from the San Fernando earthquake give values greater by as much as a factor of four than predicted by attenuation relationships derived from general strong-motion data sets. The engineering consequences of these large motions need to be considered for structures with periods of 3 sec and greater and perhaps also for structures of shorter elastic periods if those periods might be lengthened to 3 sec or beyond by deformation during an earthquake.

The results presented here also indicate the necessity of including anelastic attenuation in attempts to model ground motion in deep sedimentary basins.

Future progress in understanding basin surface waves and in predicting their amplitude will require additional data. Taking full advantage of moderate earthquakes to obtain additional data will require that operators of strong-motion networks take special care for the faithful recording of the long-period components of ground motion. Not only are instruments of sufficient dynamic range needed, but also

testing should be done to insure that sufficiently low noise levels are actually achieved. It is also necessary to insure that the recorder, once triggered, will continue to operate for a time sufficient for the surface waves to traverse the basin. With velocities of about 1 km/sec, that time may be as long as 100 sec.

6. ACKNOWLEDGMENTS

The author benefited from discussions with David Boore, John Tinsley, and Jerry Eaton. He is also grateful to Linda Seekins for her skilled efforts in making Figure 2 and to David Boore for his review of the manuscript and valuable suggestions for improvement.

7. REFERENCES

- Abrahamson, N. A. and W. J. Silva (1997). Empirical response spectral attenuation relations for shallow crustal earthquakes, *Seism. Res. Lett.*, **68**, 94-127.
- Converse, A. M. (1992). BAP: basic strong-motion accelerogram processing software; version 1.0, *U.S. Geol. Survey Open-File Rept. 92-296A*.
- Hanks, T. C. (1975). Strong ground motion of the San Fernando, California, earthquake: ground displacements, *Bull. Seism. Soc. Am.*, **65**, 193-225.
- Hanks, T. C. and R. K. McGuire (1981). The character of high-frequency strong ground motion, *Bull. Seism. Soc. Am.*, **71**, 2071-2095.
- Heaton, T. H. and D. V. Helmberger (1979). Generalized ray models of the San Fernando earthquake, *Bull. Seism. Soc. Am.*, **69**, 1311-1341.
- Joyner, W. B. and D. M. Boore (1982). Prediction of earthquake response spectra, *U.S. Geol. Survey Open-File Rept. 82-977*.
- Liu, H.-L. and T. H. Heaton (1984). Array analysis of the ground velocities and accelerations from the 1971 San Fernando,

California, earthquake, *Bull. Seism. Soc. Am.*, **74**, 1951-1968.

Seekins, L. C., A. G. Brady, C. Carpenter, and N. Brown (1992). Digitized strong-motion accelerograms of North and Central American earthquakes 1933-1986, *U.S. Geol. Survey Digital Data Series DDS-7*.

Vidale, J. E. and D. V. Helmberger (1988). Elastic finite-difference modeling of the 1971

San Fernando, California earthquake, *Bull. Seism. Soc. Am.*, **78**, 122-141.

Yerkes, R. F., T. H. McCulloh, J. E. Schoellhamer, and J. G. Vedder (1965). Geology of the Los Angeles Basin California – an introduction, *U.S. Geol. Survey Prof. Paper 420-A*, 57 p.

Table 1. Values of a and b obtained by fitting equation (1) to data from the San Fernando and Northridge earthquakes.

San Fernando earthquake

Period (sec)	a			b		
	Perpendicular	Parallel	Vertical	Perpendicular	Parallel	Vertical
3.0	741	581	341	0.0190	0.0205	0.0097
4.0	791	883	393	0.0139	0.0156	0.0064
5.0	690	887	265	0.0115	0.0075	-0.0001
6.0	514	644	167	0.0090	0.0045	0.0010

Northridge earthquake

Period (sec)	a			b		
	Perpendicular	Parallel	Vertical	Perpendicular	Parallel	Vertical
3.0	327	541	286	0.0116	0.0222	0.0241
4.0	254	488	238	0.0103	0.0166	0.0207
5.0	169	266	156	0.0001	0.0118	0.0167
6.0	132	195	112	0.0026	0.0109	0.0147

Table 2. Values of Q implied by the b values in Table 1, with one-standard-deviation ranges, for an assumed phase velocity of 1 km/sec.

San Fernando earthquake

Period (sec)	Perpendicular	Parallel	Vertical
3.0	55 (45-73)	51 (43-63)	110 (77-180)
4.0	56 (46-72)	50 (41-66)	120 (72-430)
5.0	55 (43-75)	84 (61-140)	∞ (180- ∞)
6.0	58 (41-99)	120 (70-360)	510 (120- ∞)

Northridge earthquake

Period (sec)	Perpendicular	Parallel	Vertical
3.0	90 (63-160)	47 (39-60)	44 (36-55)
4.0	76 (52-140)	47 (36-69)	38 (30-50)
5.0	5300 (140- ∞)	53 (37-91)	38 (29-53)
6.0	200 (78- ∞)	48 (34-84)	36 (28-49)

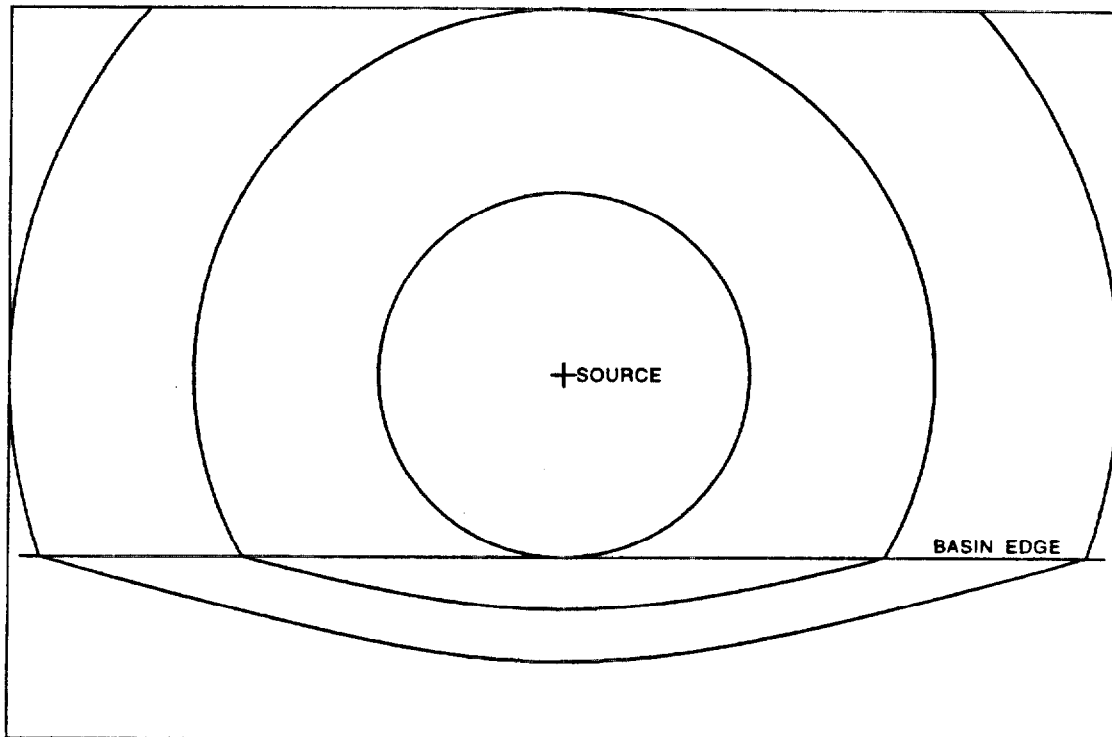


Figure 1. Schematic plan view of the wavefronts for an S wave from a point source converting to a surface wave at the edge of a basin. The phase velocity of the surface wave is one-third the S wave velocity.

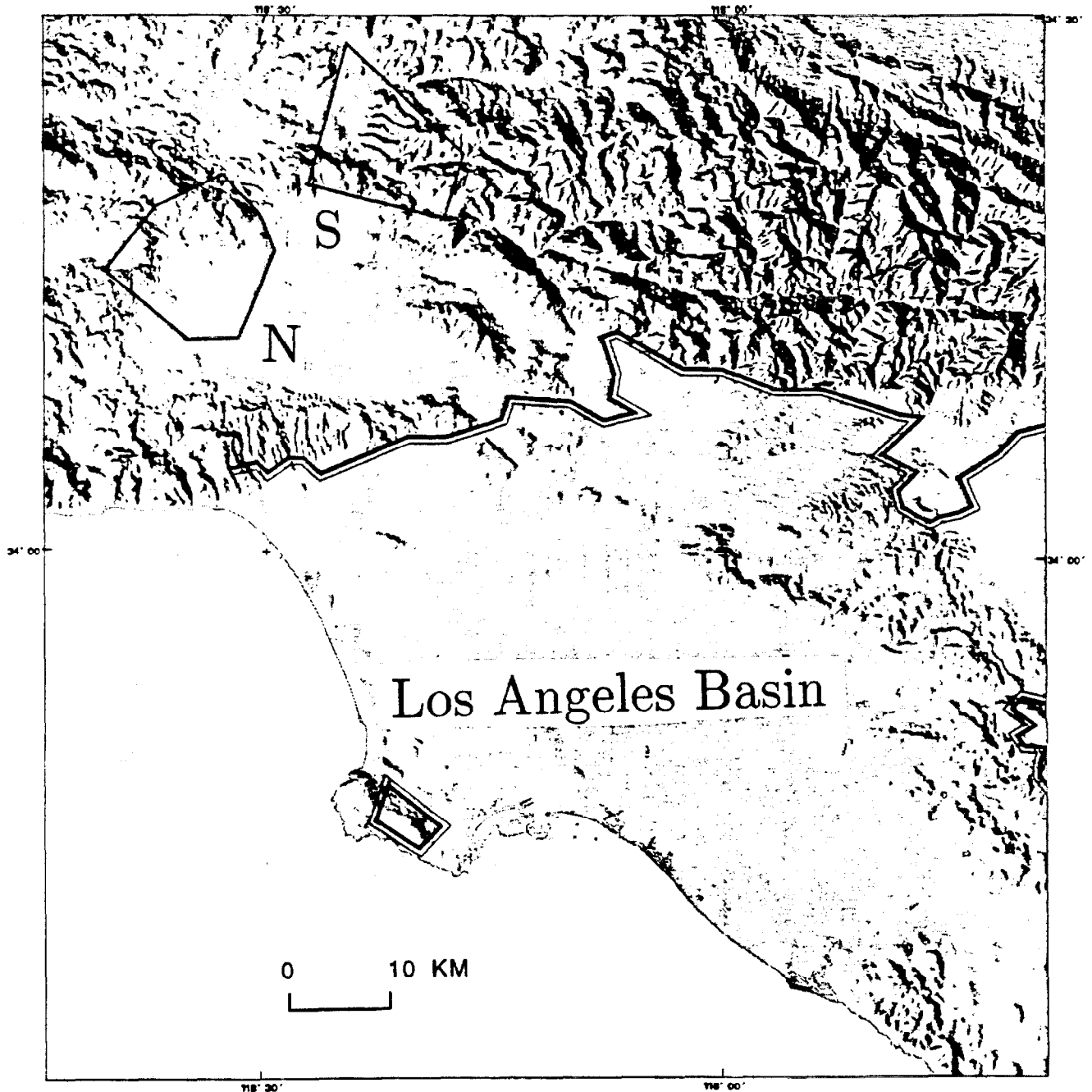


Figure 2. Map showing the boundary of the Los Angeles Basin (double line) as defined in the text. Polygons outline the vertical projection of the rupture surface in the San Fernando earthquake (S) (Heaton and Helmberger, 1979) and the Northridge earthquake (N) (David Wald, written communication, 1995).

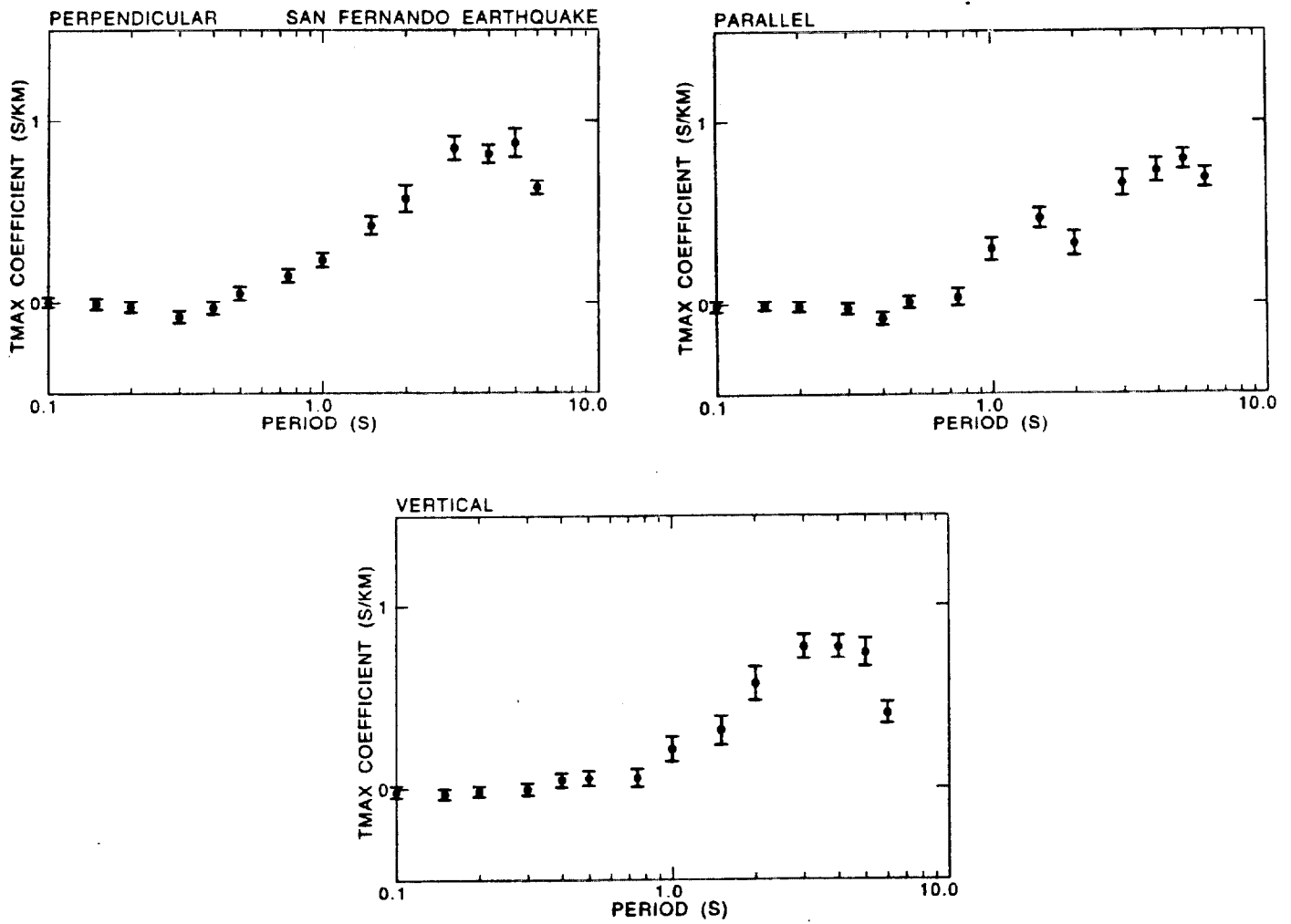


Figure 3. Regression coefficient between the time of maximum pseudovelocity response and closest horizontal distance to the vertical projection of the fault rupture for records from the San Fernando earthquake. The bars show the one-standard-error range for the coefficient.

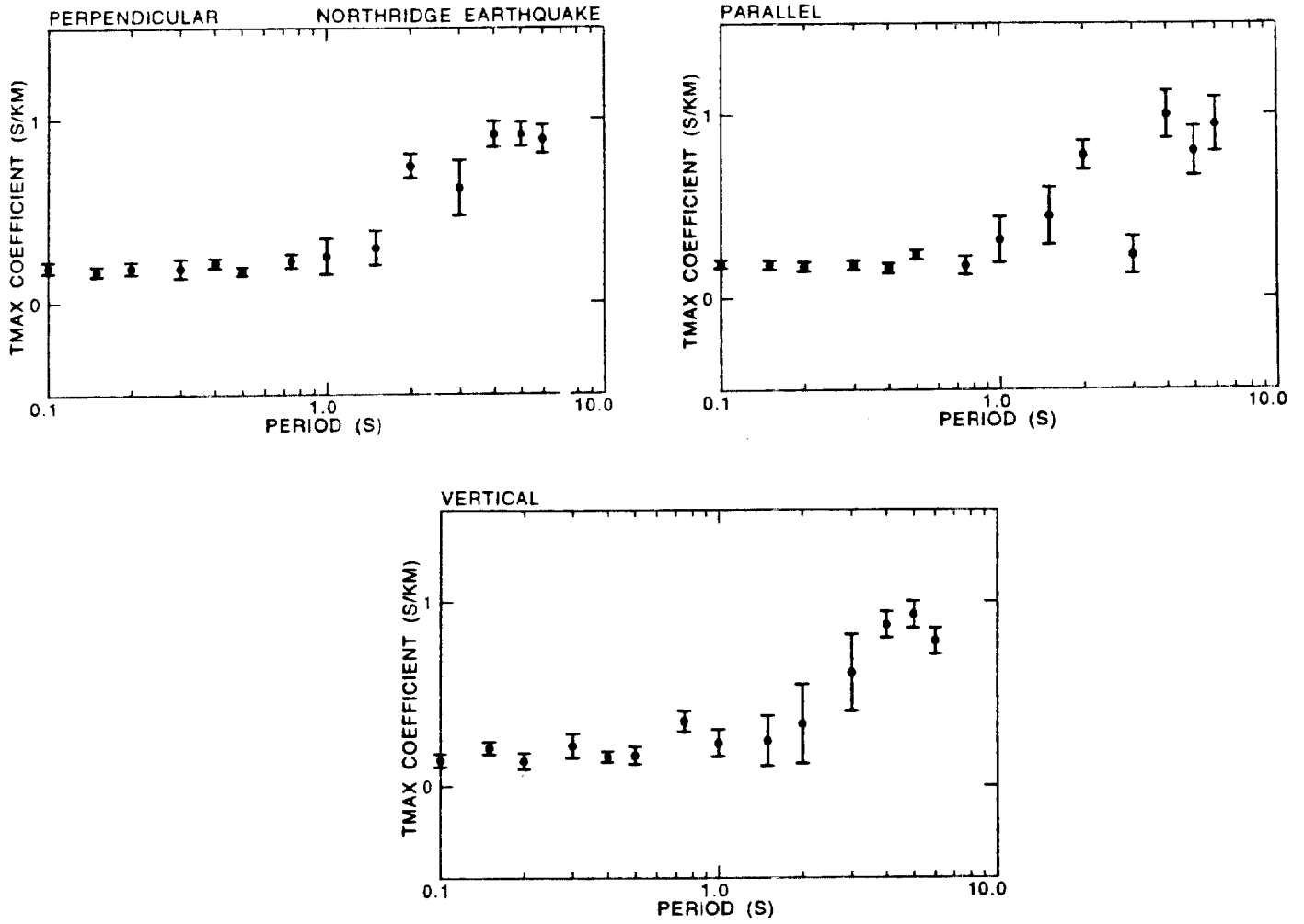


Figure 4. Regression coefficient between the time of maximum pseudovelocity response and closest horizontal distance to the vertical projection of the fault rupture for records from the Northridge earthquake. The bars show the one-standard-error range for the coefficient.

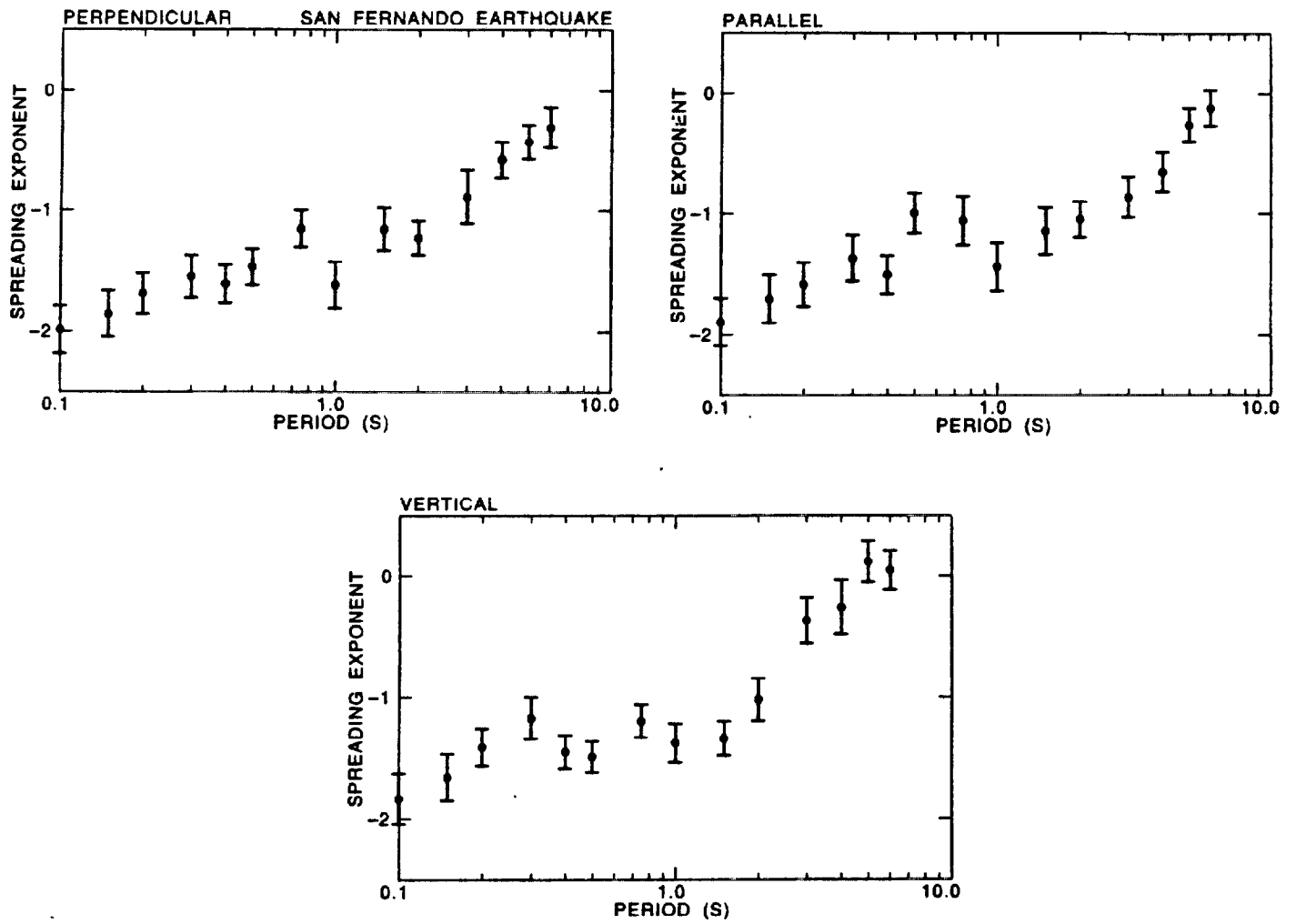


Figure 5. Regression coefficient between the logarithm of pseudovelocity response and the logarithm of closest horizontal distance to the vertical projection of the fault rupture for records from the San Fernando earthquake. The bars show the one-standard-error range for the coefficient.

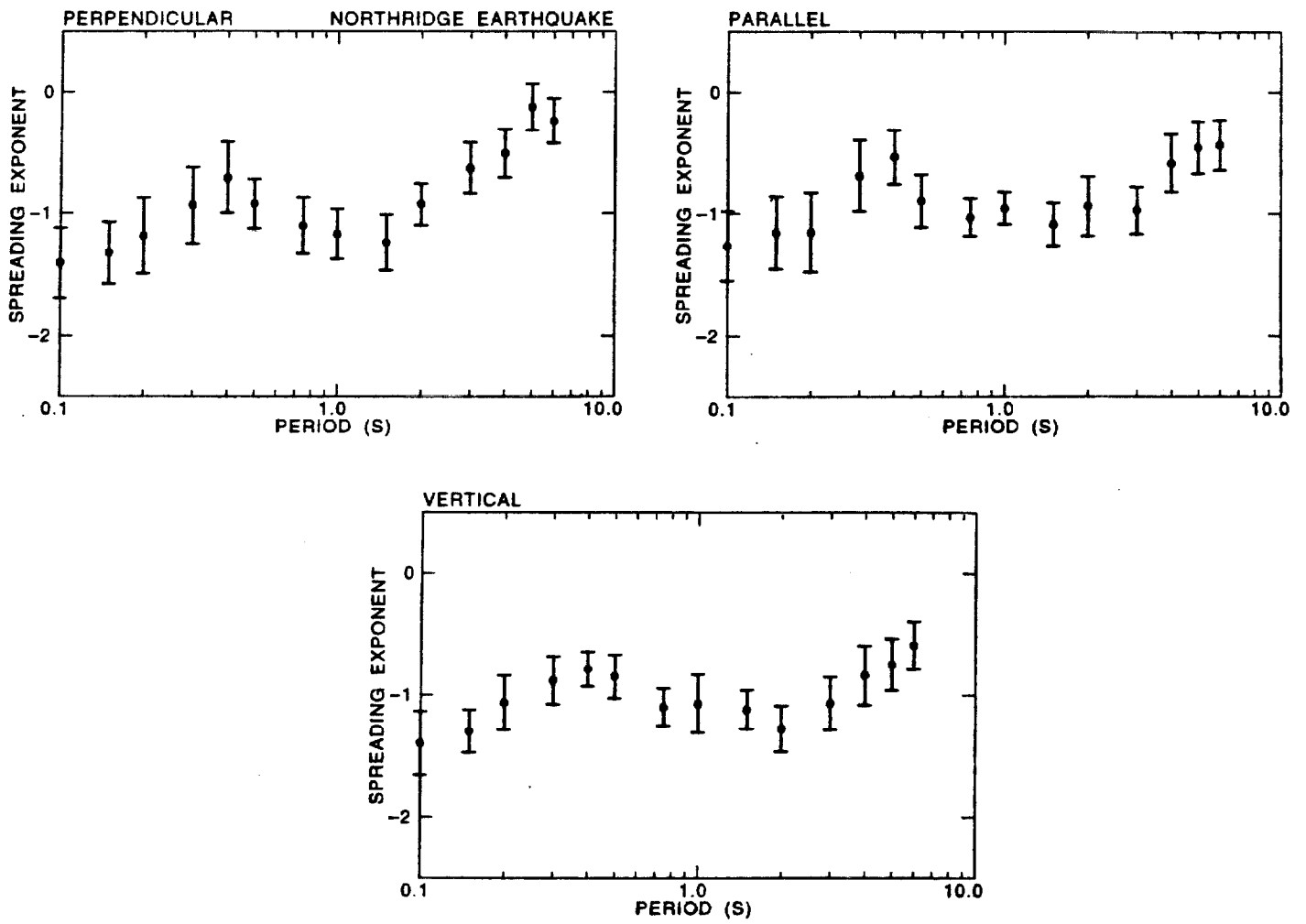


Figure 6. Regression coefficient between the logarithm of pseudovelocity response and the logarithm of closest horizontal distance to the vertical projection of the fault rupture for records from the Northridge earthquake. The bars show the one-standard-error range for the coefficient.

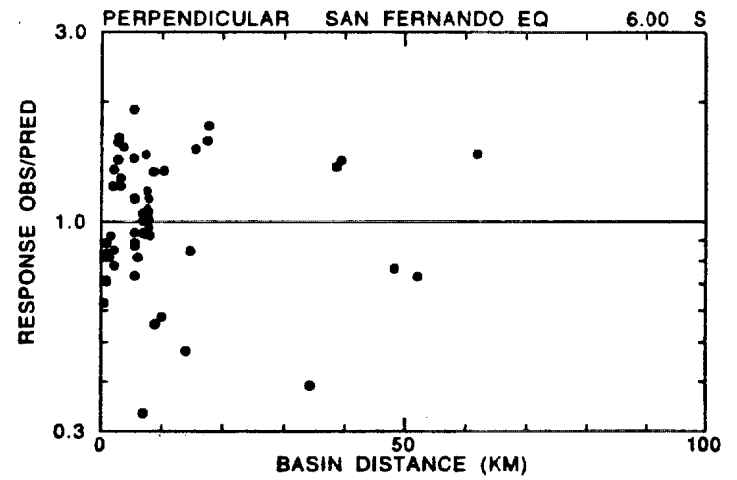
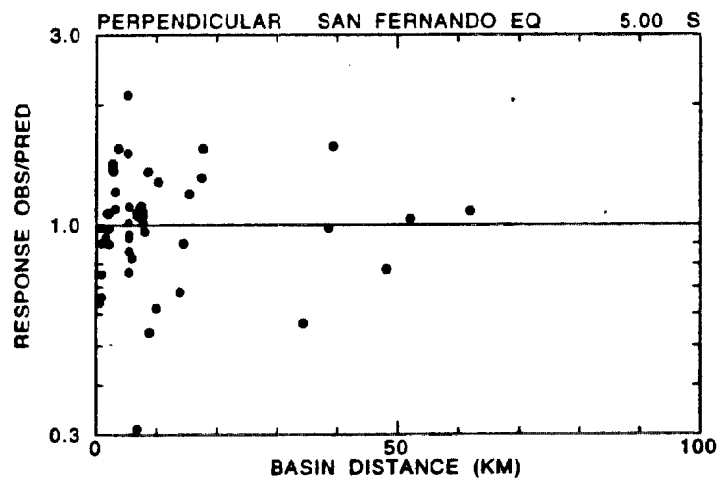
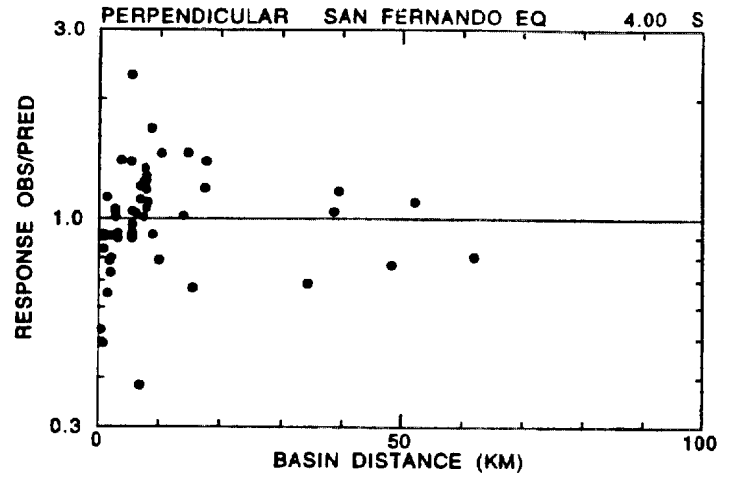
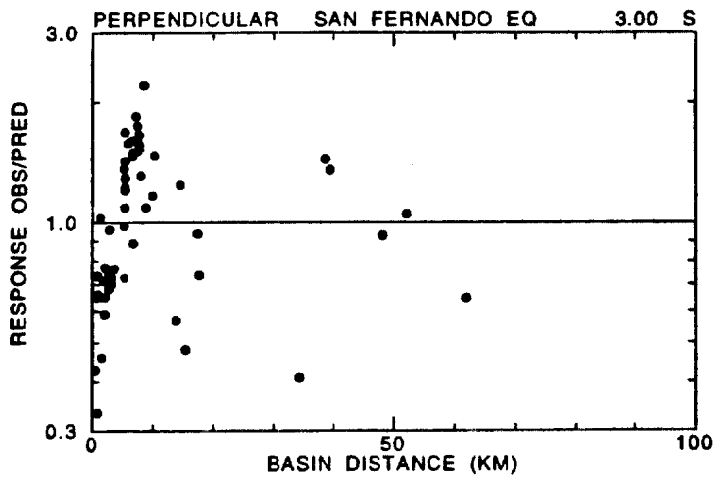


Figure 7. Ratios between observed values of pseudovelocity response and values predicted by equation (1) for the perpendicular component of the San Fernando earthquake.

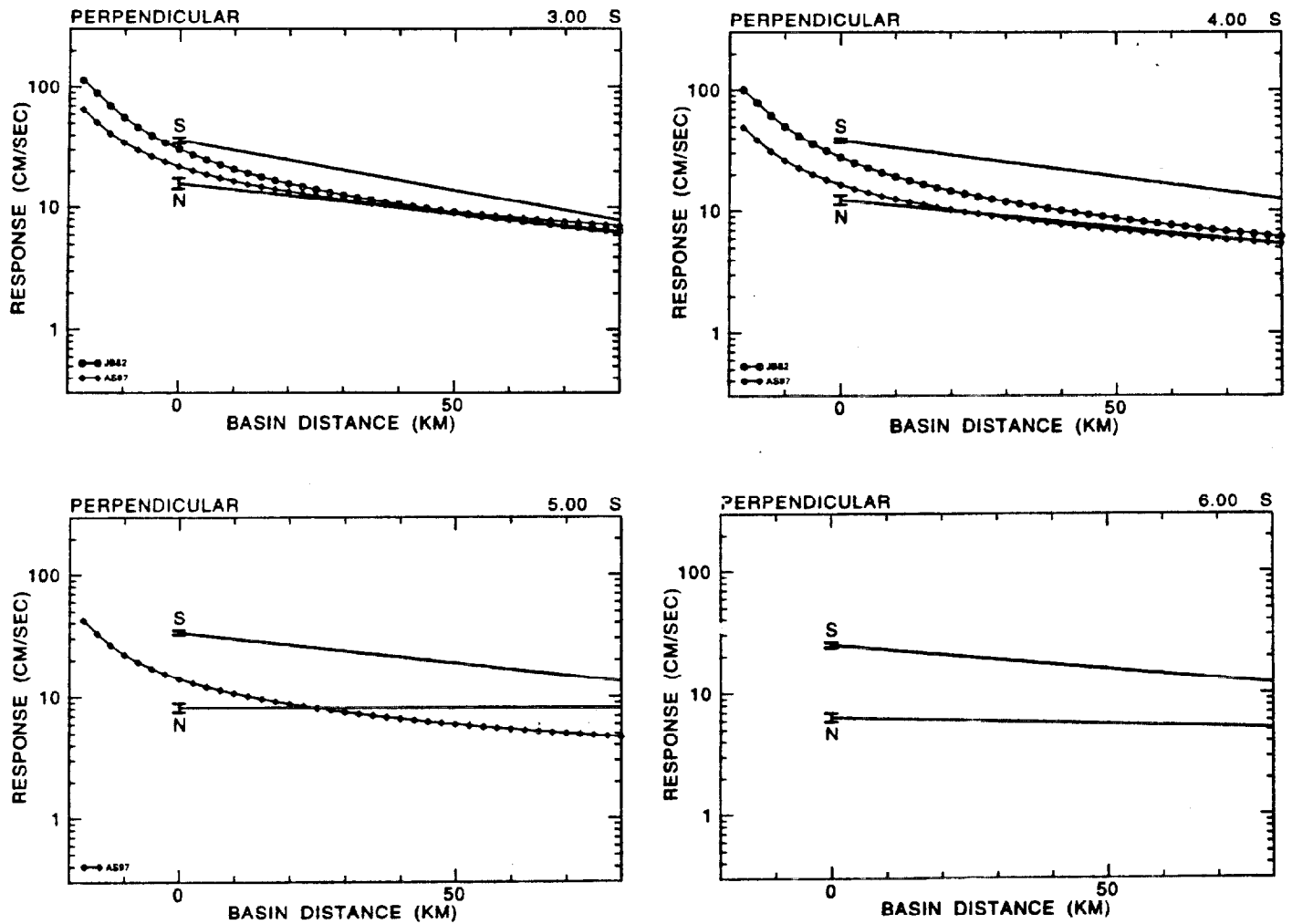


Figure 8. Values of pseudovelocity response for the perpendicular component predicted by equation (1) with coefficients fitted to data from the San Fernando earthquake (S) and the Northridge earthquake (N). The bars show the one-standard-error range for the coefficient a . Also shown are the values predicted by the equations of Joyner and Boore (1982) for soil sites (JB82) and the equations of Abrahamson and Silva (1997) for soil sites and reverse-fault earthquakes (AS97). A moment magnitude of 6.7 and a basin edge distance of 20 km were assumed for the JB82 and AS97 curves.

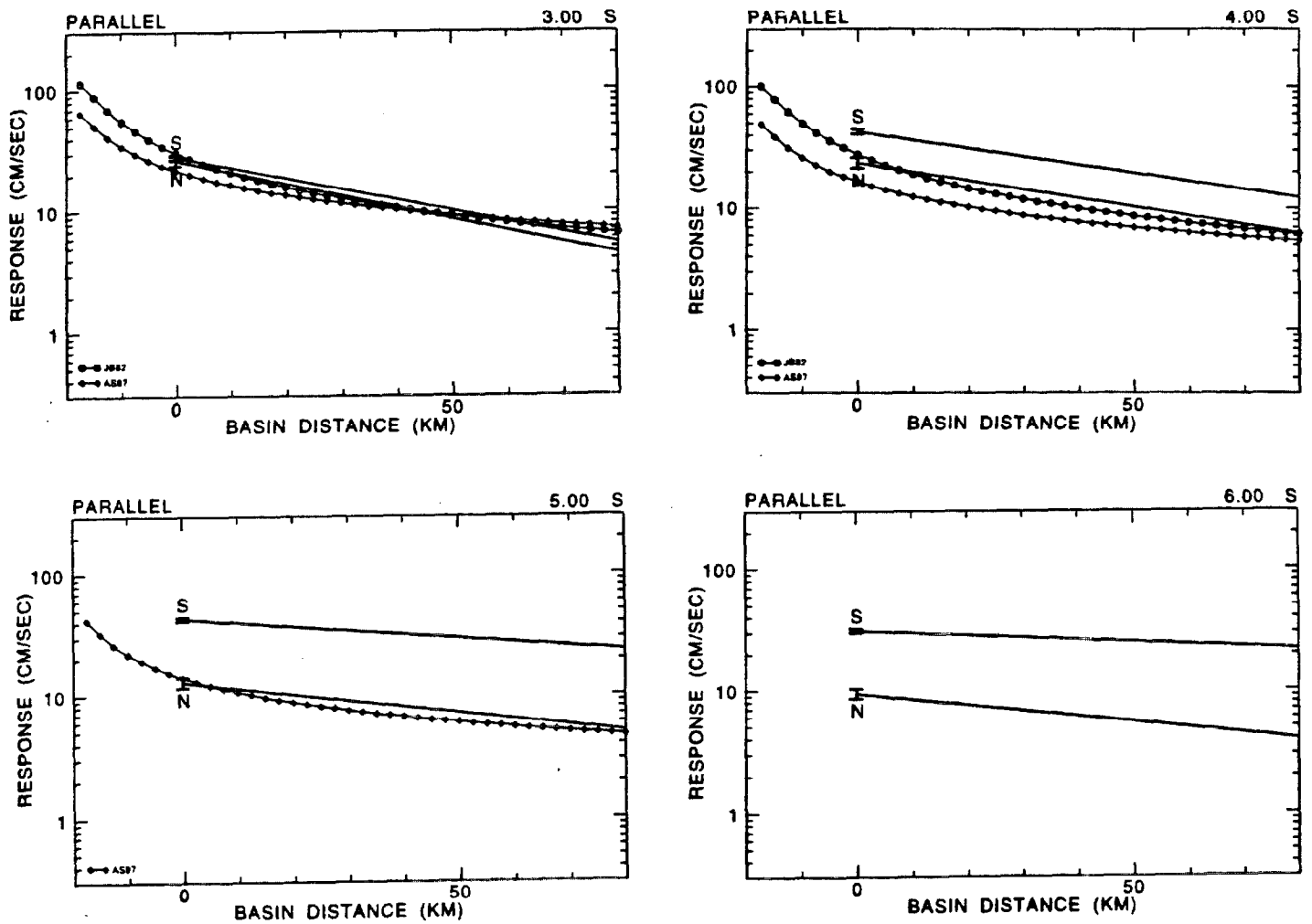


Figure 9. Values of pseudovelocity response for the parallel component predicted by equation (1) with coefficients fitted to data from the San Fernando earthquake (S) and the Northridge earthquake (N). The bars show the one-standard-error range for the coefficient a . Also shown are the values predicted by the equations of Joyner and Boore (1982) for soil sites (JB82) and the equations of Abrahamson and Silva (1997) for soil sites and reverse-fault earthquakes (AS97). A moment magnitude of 6.7 and a basin edge distance of 20 km were assumed for the JB82 and AS97 curves.